catalysts

MDPI

Supplementary materials

Revisiting the Semi-hydrogenation of Phenylacetylene to Styrene over Palladium-Lead Alloyed Catalysts on Precipitated Calcium Carbonate Supports

Yifan Zheng [1,†], Lin Gu [1,†], Yining Li [1,†], Jamal Ftouni [2], Abhishek Dutta Chowdhury [1,*]

Section S1 | Supplementary Figures

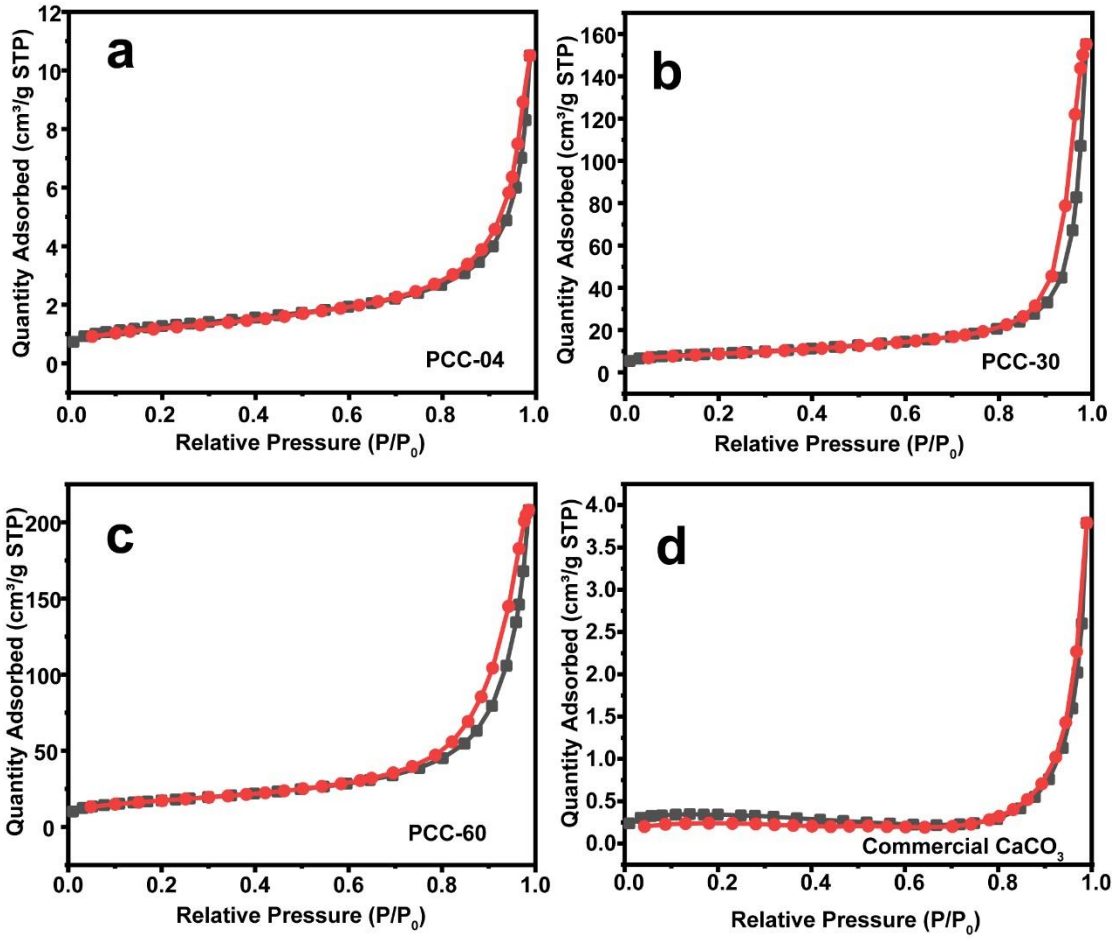

Figure S1. The physical adsorption spectrum of the (**a**) PCC-04, (**b**) PCC-30, (**c**) PCC-60, and (**d**) commercial $CaCO_3$.

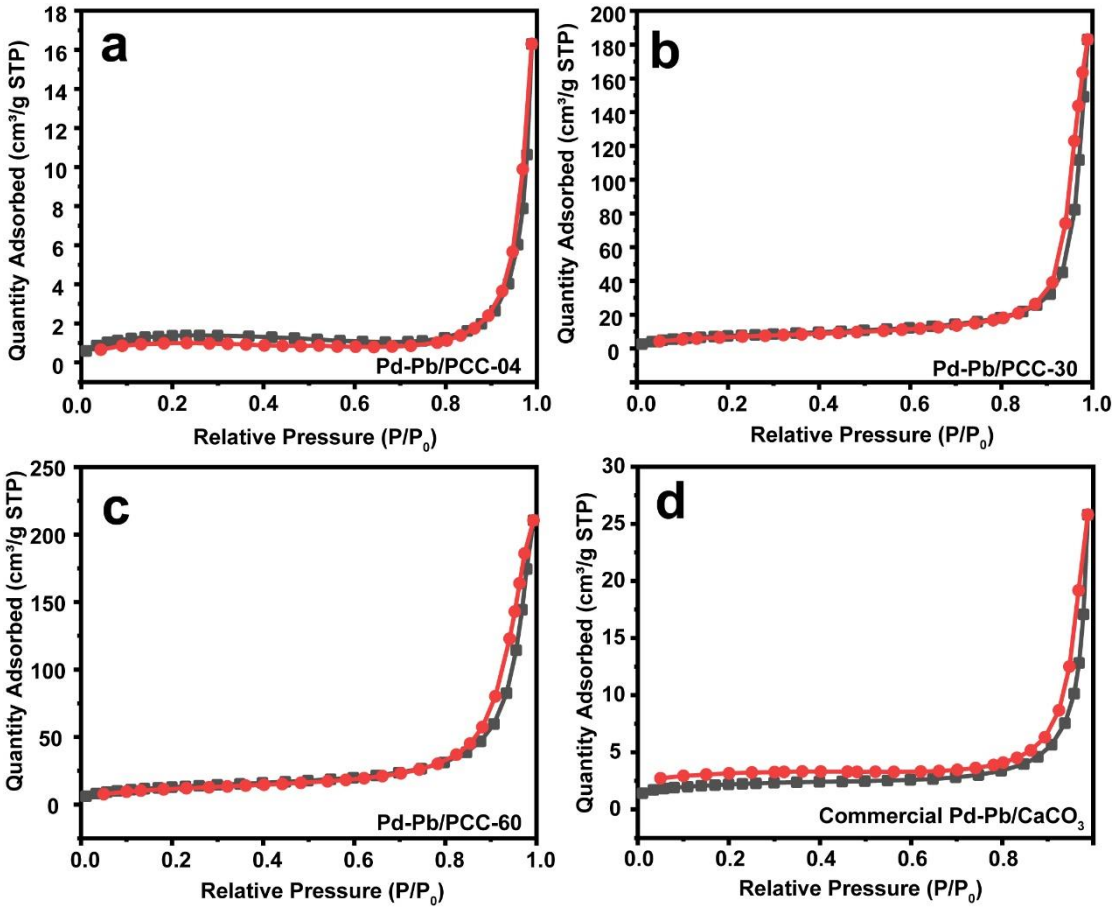

Figure S2. The physical adsorption spectrum of 5 wt% (**a**) Pd-Pb/PCC-04, (**b**) Pd-Pb/PCC-30, (**c**) Pd-Pb/PCC-60, and (**d**) commercial Pd-Pb/$CaCO_3$ (Lindlar catalyst).

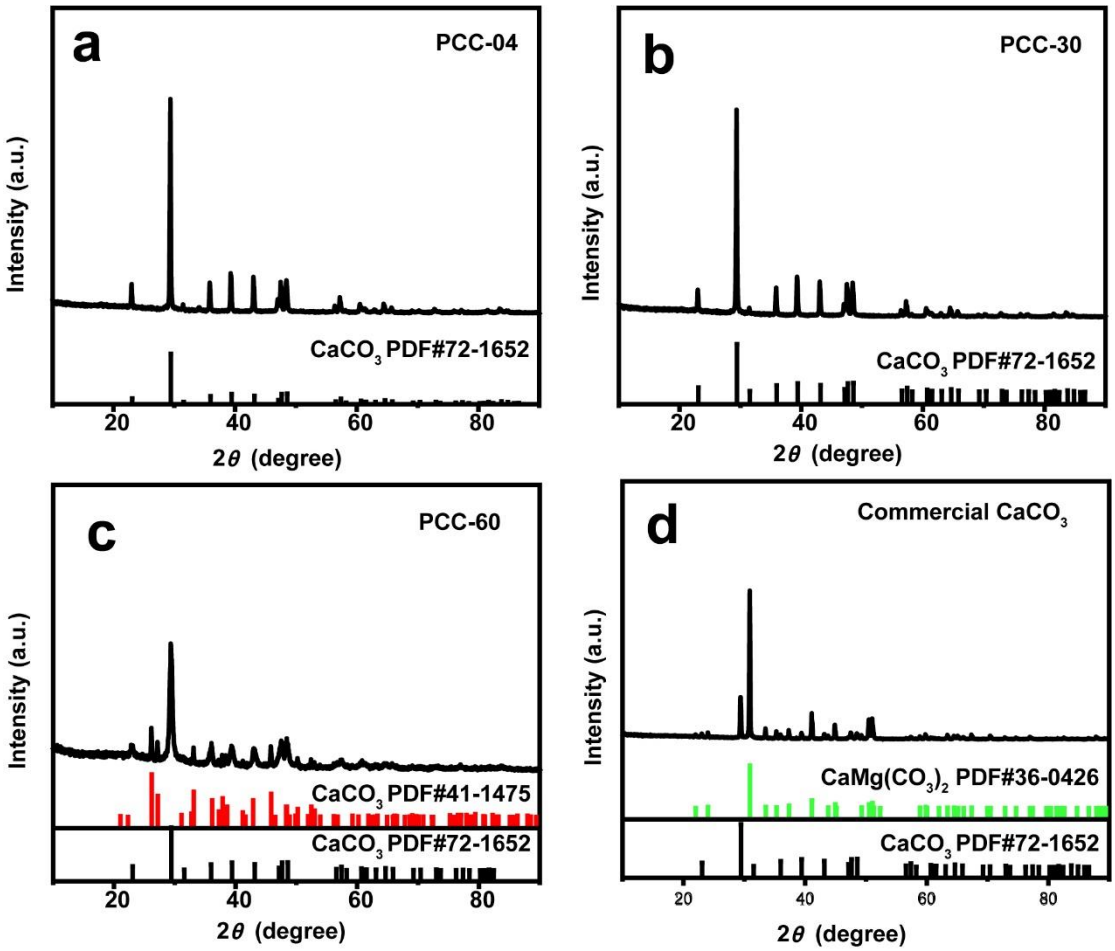

Figure S3. The XRD spectrum of the (**a**) PCC-04, (**b**) PCC-30, (**c**) PCC-60, and (**d**) commercial $CaCO_3$. (PDF#72-1652 belongs to calcite, PDF#41-1475 belongs to aragonite, PDF#36-0426 belongs to $CaMg(CO)_3$). Herein for PCC-60 support, the intensity of any characteristic diffraction peaks is proportional to the content of respective phases since the material does not have any preferred orientation. Under the same density, analyzing the intensity of their characteristic diffraction peaks could analyze the content of different phases in the standalone PCC-60 supports, which we perform according to the adiabatic method equation.

$$Wa = \frac{1}{1 + \frac{Ka}{Kc} / \frac{Ia}{Ic}} \qquad Wc = \frac{1}{1 + \frac{Kc}{Ka} / \frac{Ic}{Ia}}$$

Where *Wa* and *Wc* represent the mass fraction of aragonite and calcite, respectively. *Ka* and *Kc* represent the reference strengths of aragonite and calcite, respectively. *Ia* and *Ic* represent the peak intensities of aragonite and calcite, respectively. Based on these calculations, the calcite component in PCC-60 accounts for 49.2%, and the aragonite component accounts for 50.8%. Hence, PCC-60 comprises almost equal contributions from both calcine and aragonite phases.

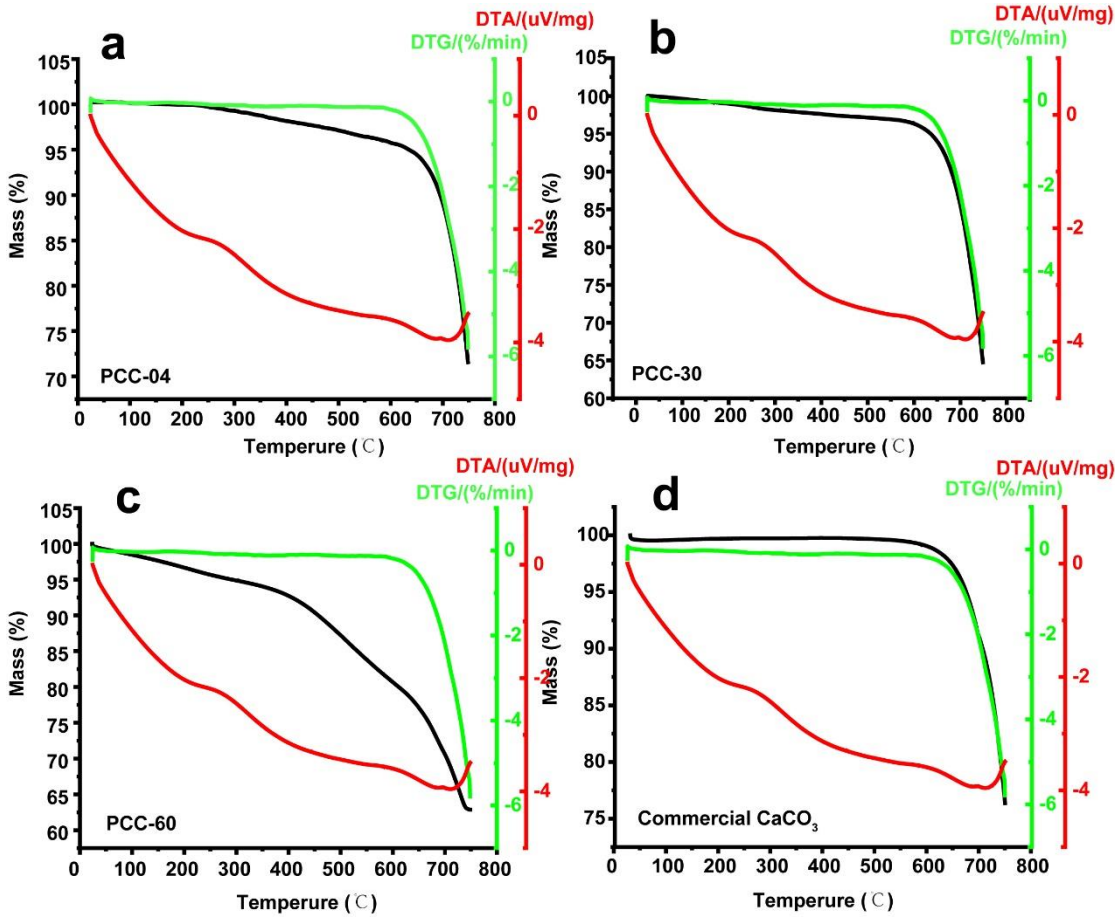

Figure S4. Thermogravimetric analysis (TGA) and differential thermal analysis (DTA) of (**a**) PCC-04, (**b**) PCC-30, (**c**) PCC-60, and (**d**) commercial $CaCO_3$.

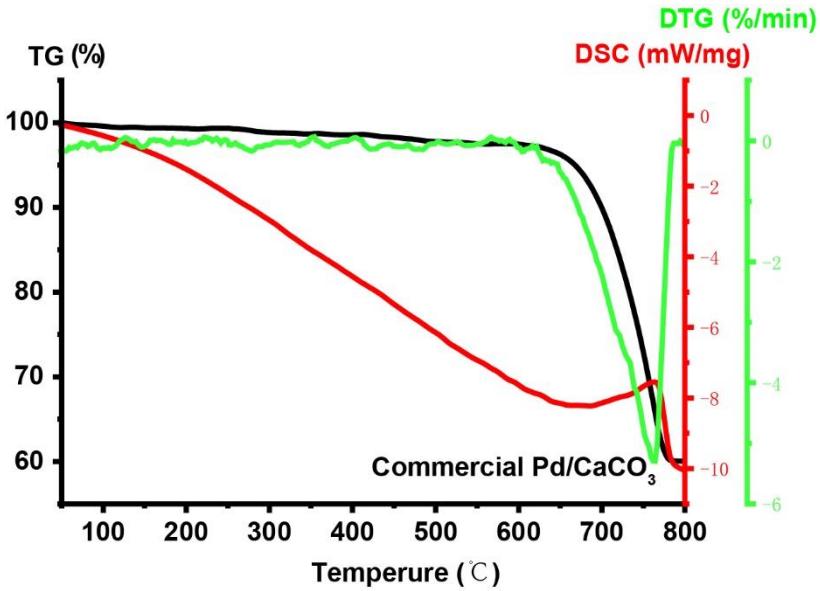

Figure S5. Thermogravimetric analysis (TGA) and differential scanning calorimetry (DSC) of the commercial 5wt% Pd-Pb/$CaCO_3$ material (Lindlar catalyst).

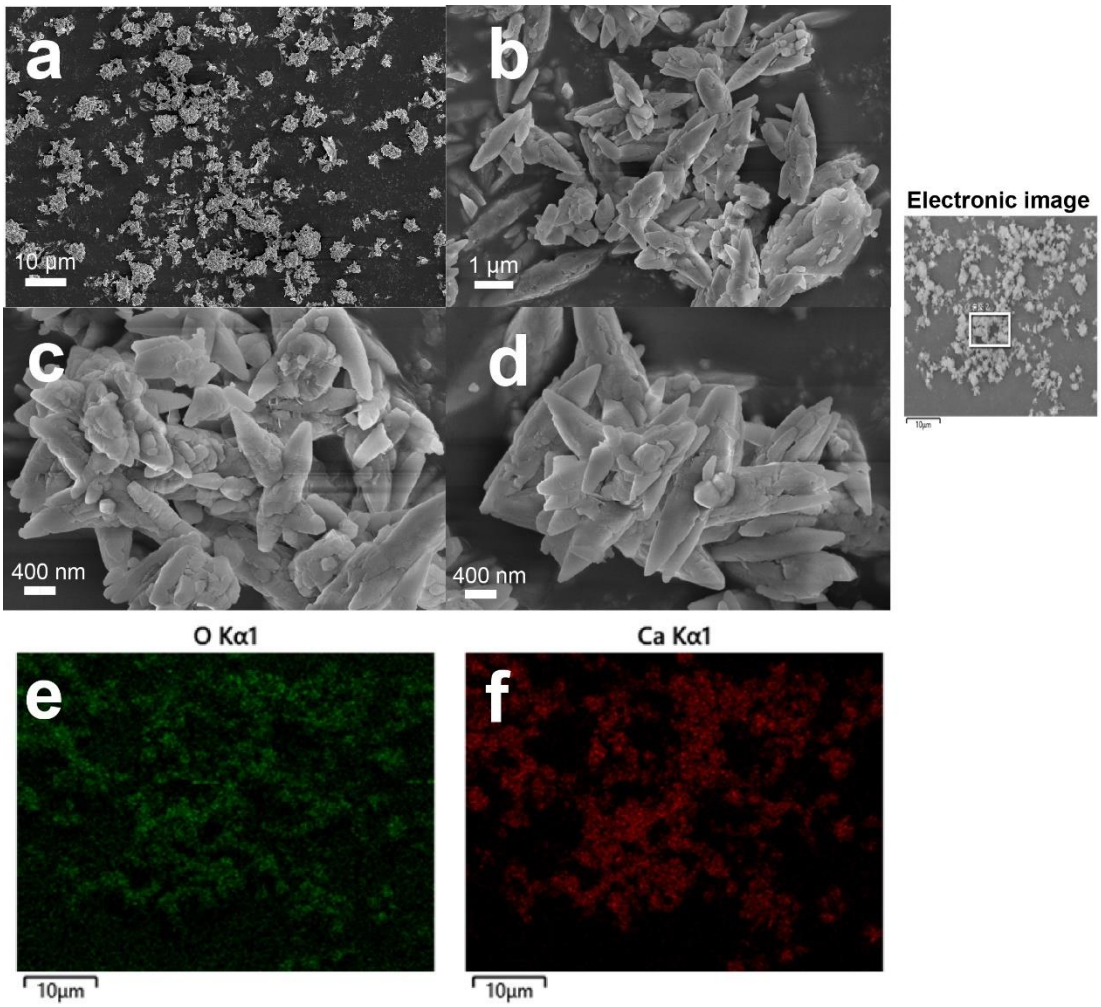

Figure S6. (**a**–**d**) Scanning electron microscope (SEM) images of standalone PCC-04 support, including mapping of (**e**) oxygen and (**f**) calcium.

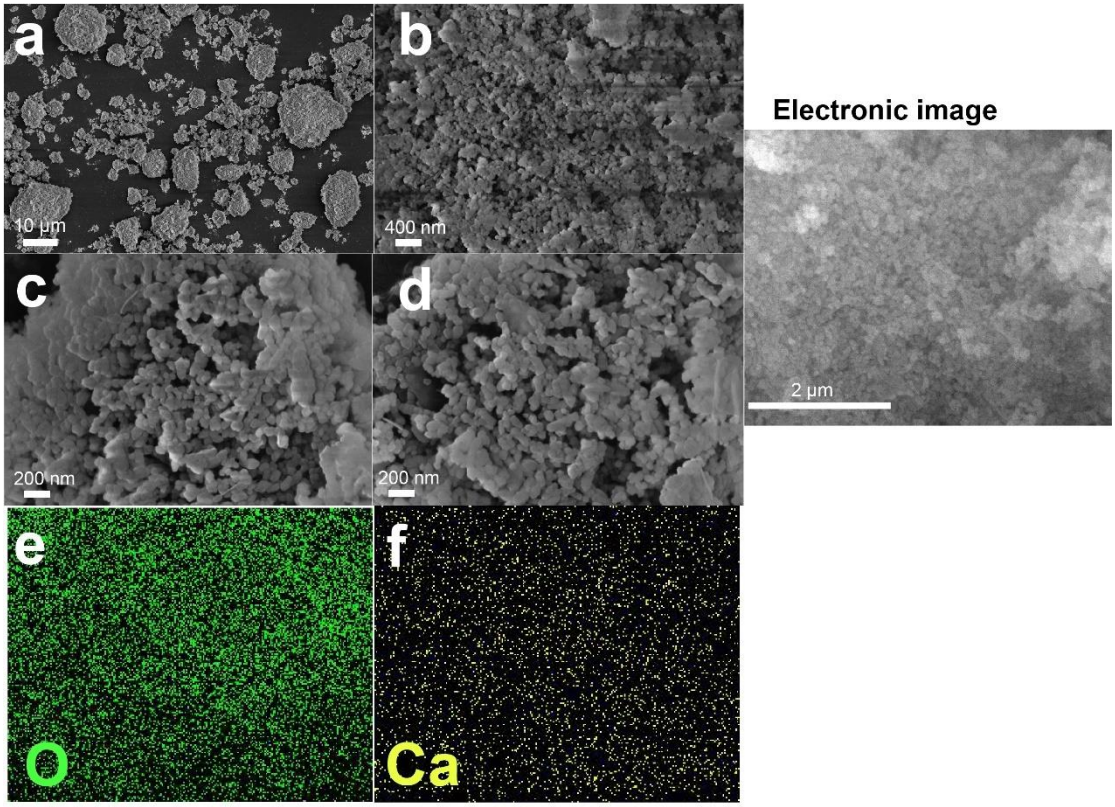

Figure S7. (**a**–**d**) Scanning electron microscope (SEM) images of standalone PCC-30 support, including mapping of (**e**) oxygen and (**f**) calcium.

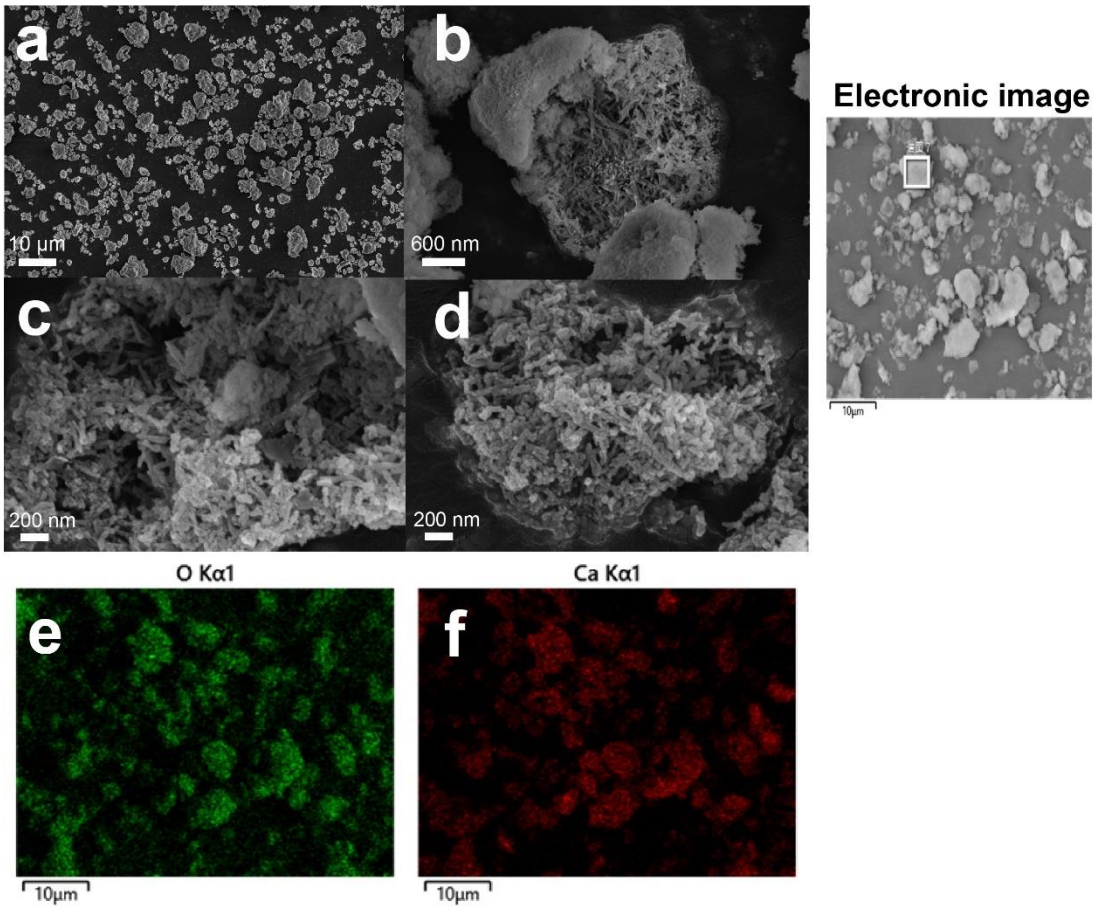

Figure S8. (**a**–**d**) Scanning electron microscope (SEM) images of standalone PCC-60 support, including mapping of (**e**) oxygen and (**f**) calcium.

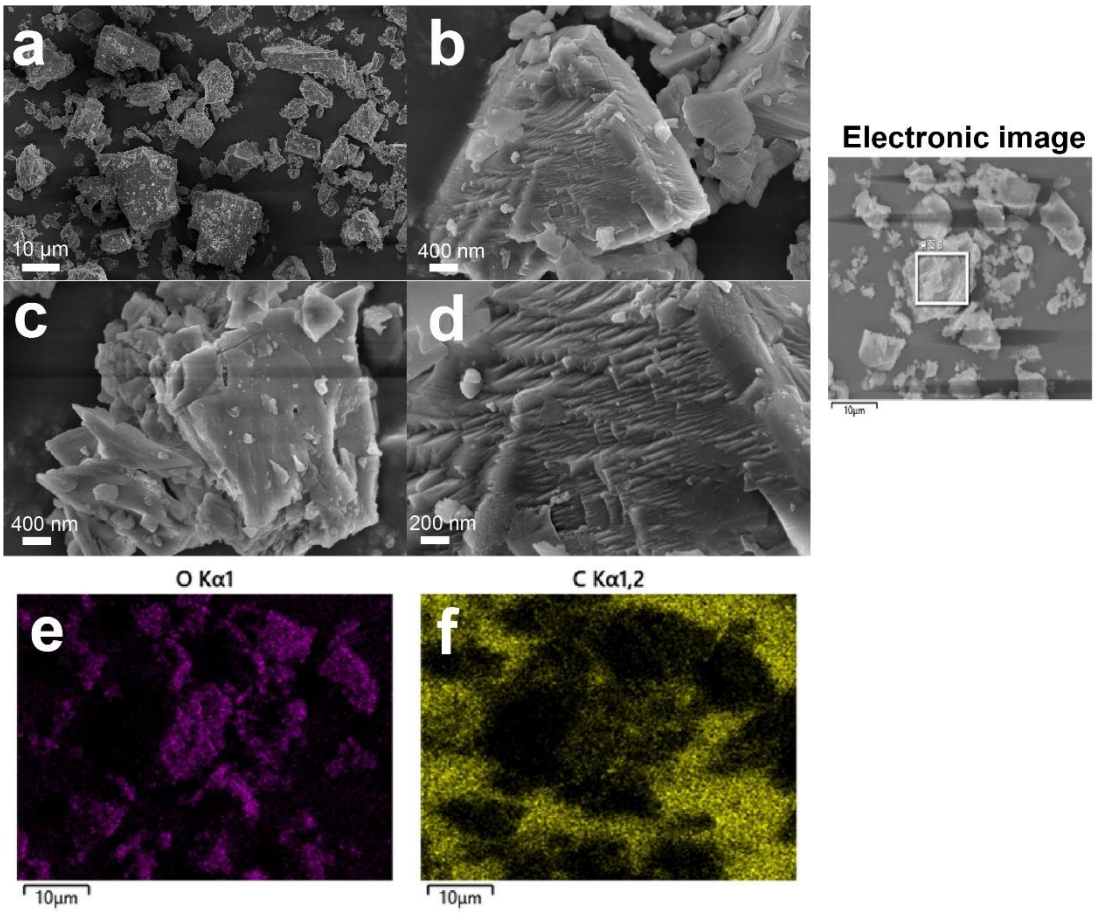

Figure S9. (**a**–**d**) Scanning electron microscope (SEM) images of standalone commercial $CaCO_3$ support, including mapping of (**e**) oxygen and (**f**) calcium.

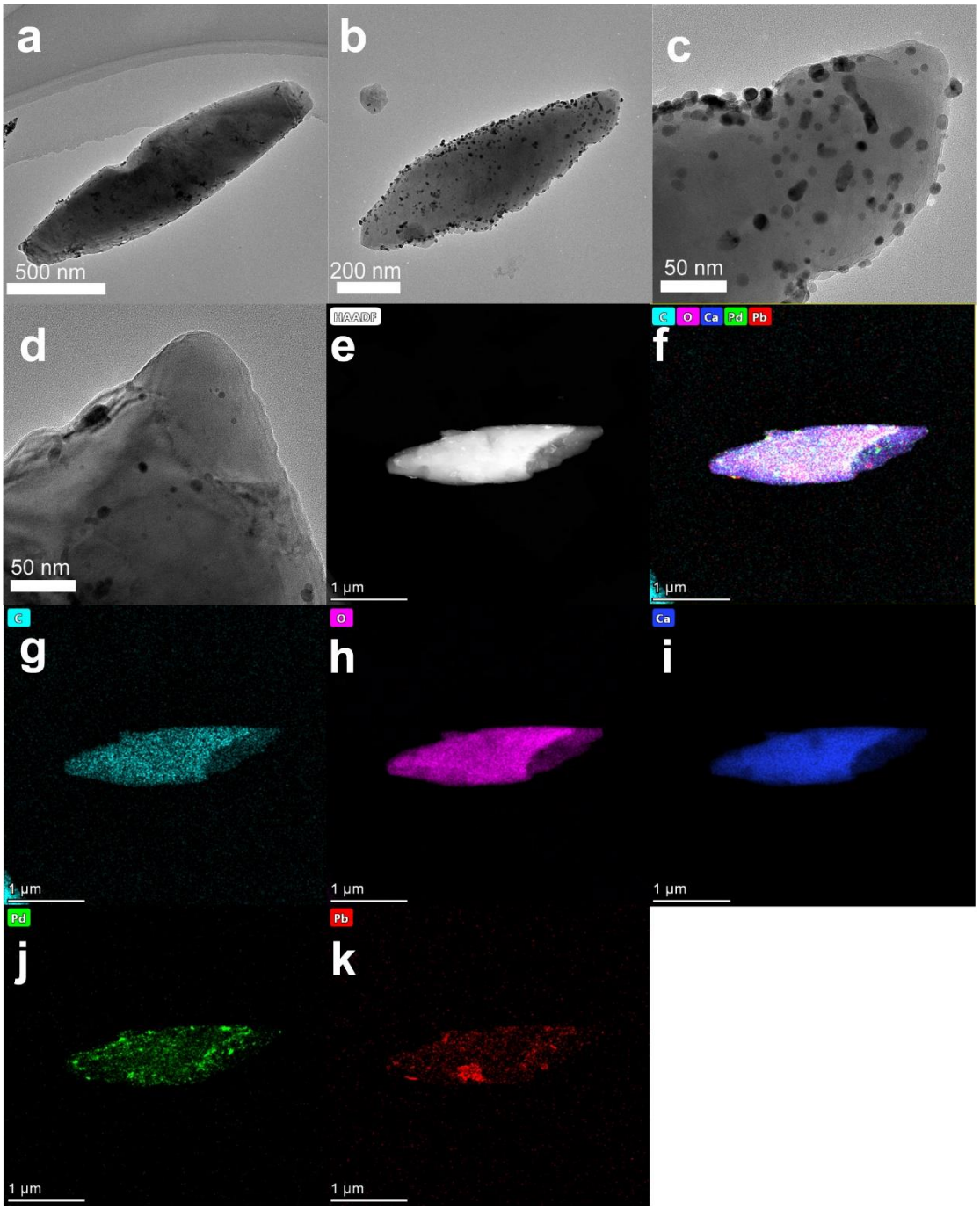

Figure S10. (**a**–**d**) Transmission Electron Microscope (TEM) images of standalone 5 wt% Pd-Pb/PCC-04, including (**e**) electronic image, (**f**) overlapping mapping of key elements, as well as individual mapping of (**g**) carbon, (**h**) oxygen, (**i**) calcium (**j**) palladium, and (**k**) lead. The particle size of palladium nanoparticles is ± 7 nm.

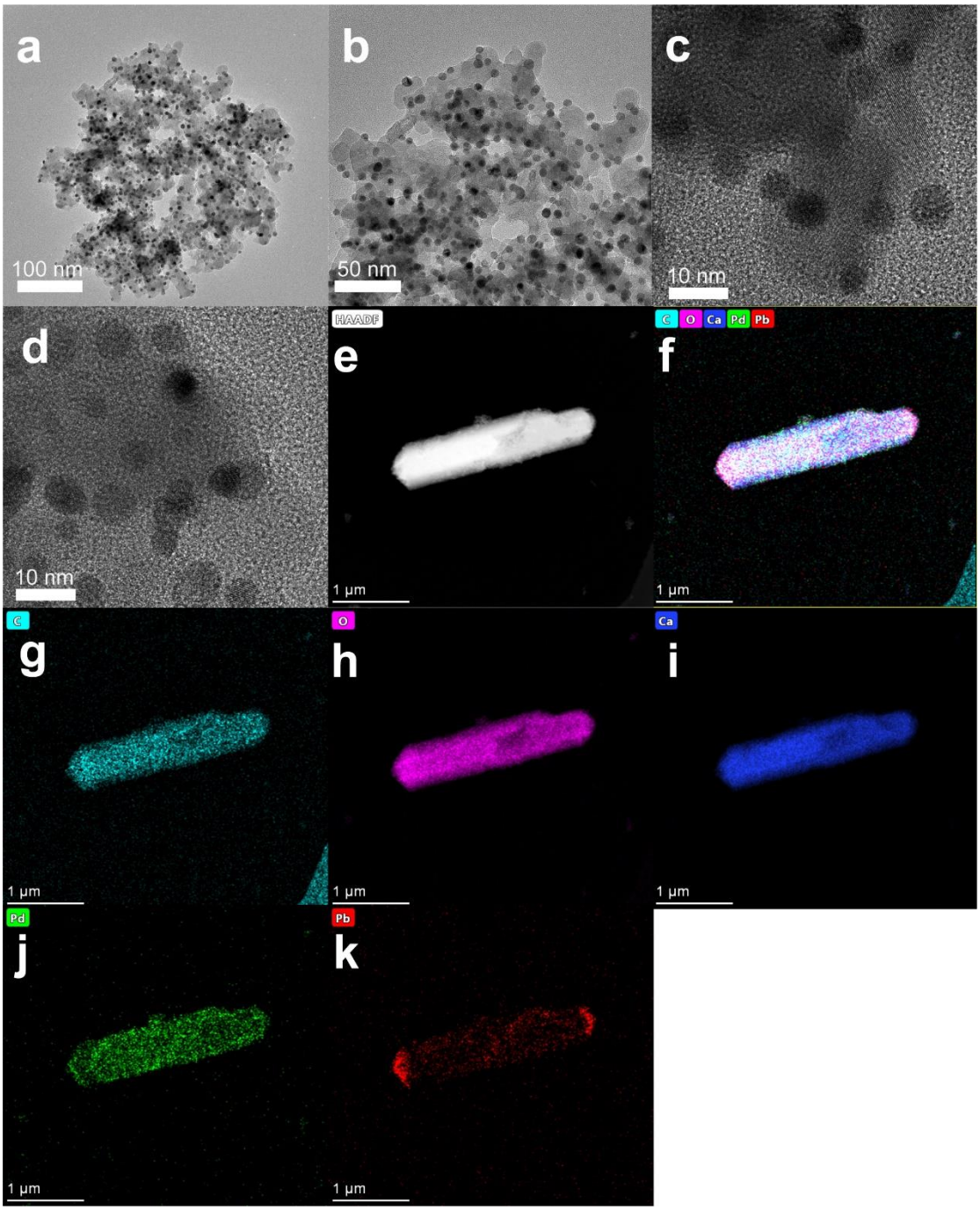

Figure S11. (**a**–**d**) Transmission Electron Microscope (TEM) images of standalone 5 wt% Pd-Pb/PCC-60, including (**e**) electronic image, (**f**) overlapping mapping of key elements, as well as individual mapping of (**g**) carbon, (**h**) oxygen, (**i**) calcium (**j**) palladium, and (**k**) lead. The particle size of palladium nanoparticles is ± 7 nm.

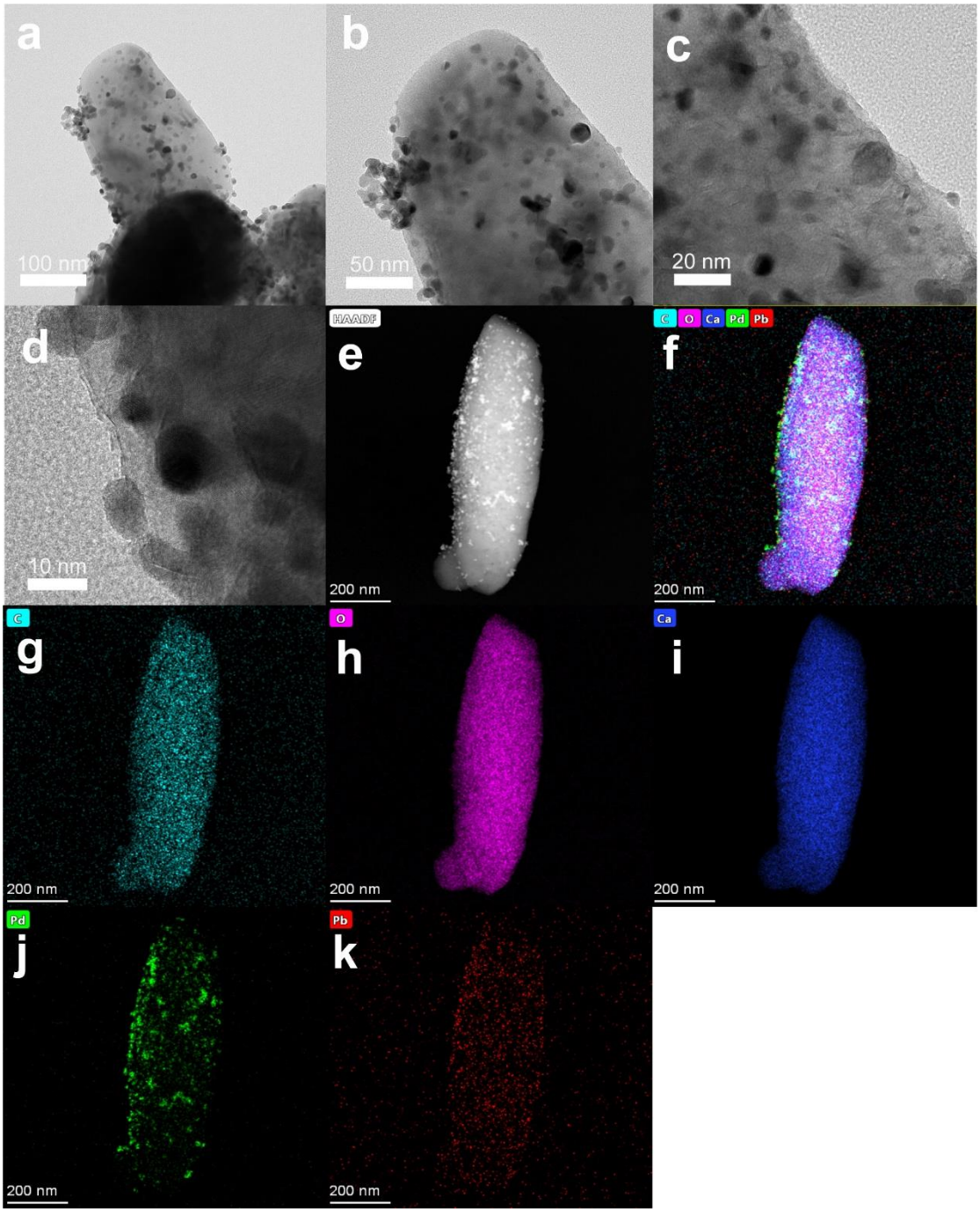

Figure S12. (**a**–**d**) Transmission Electron Microscope (TEM) images of commercial 5 wt% Pd-Pb/$CaCO_3$ (i.e., Lindlar), including (**e**) electronic image, (**f**) overlapping of key elements, as well as individual mapping of (**g**) carbon, (**h**) oxygen, (**i**) calcium (**j**) palladium, and (**k**) lead. The particle size of palladium nanoparticles is ± 6 nm.

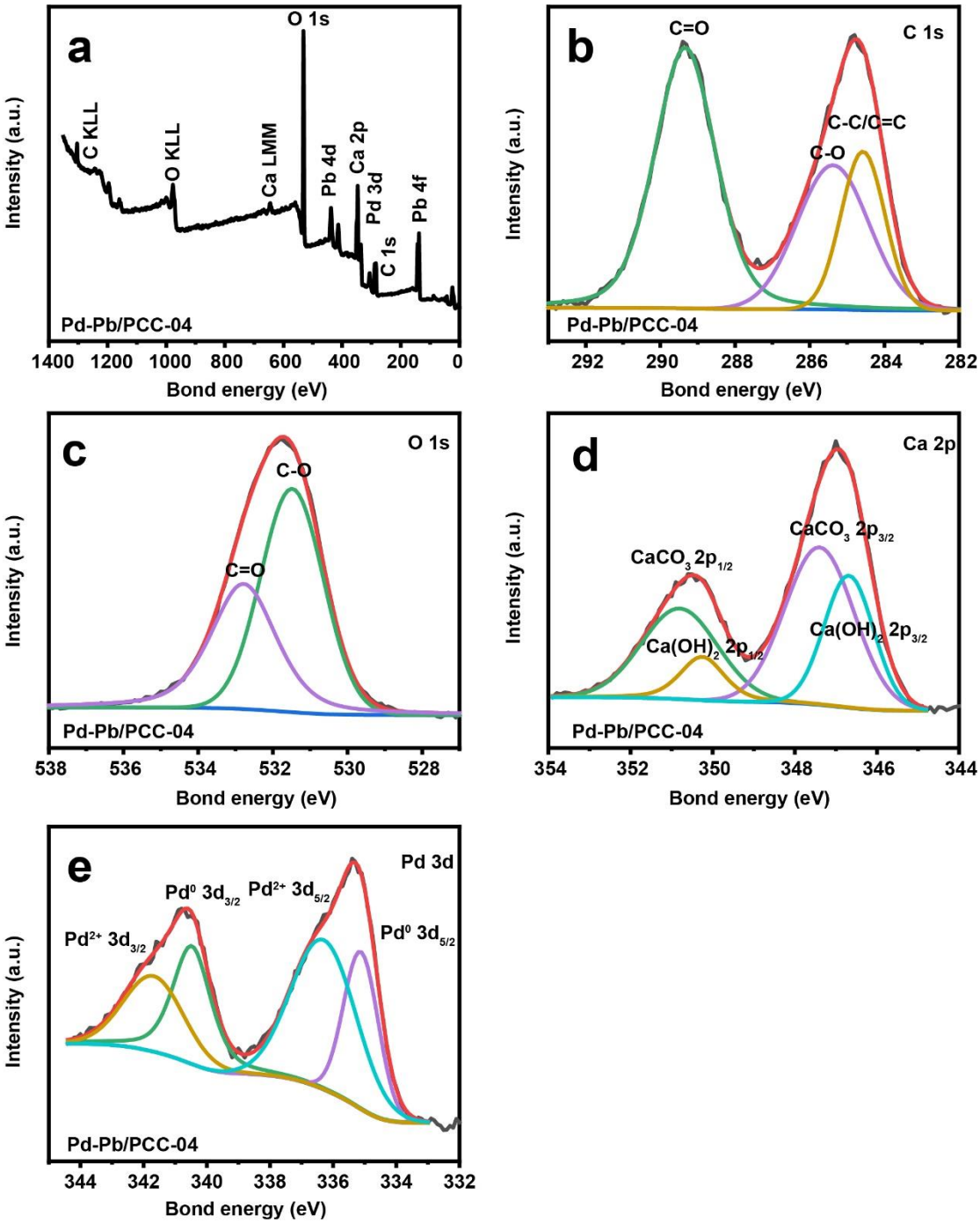

Figure S13. X-ray photoelectron spectroscopy (XPS) profiles of 5 wt% Pd-Pb/PCC-04 material, including (**a**) full spectrum, (**b**) C 1s, (**c**) O 1s, (**d**) Ca 2p and (**e**) Pd 3d.

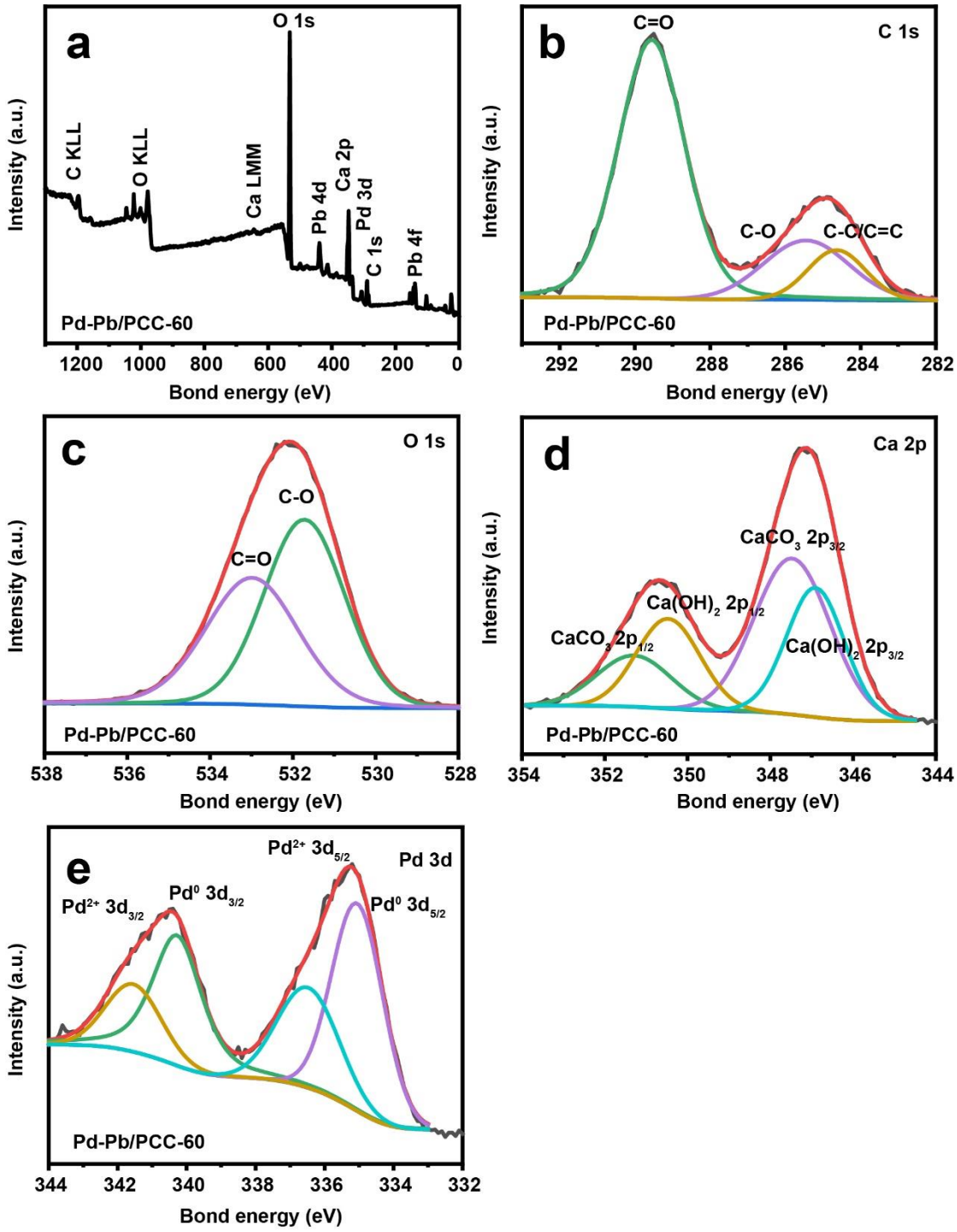

Figure S14. X-ray photoelectron spectroscopy (XPS) profiles of 5 wt% Pd-Pb/PCC-60, including (**a**) full spectrum, (**b**) C 1s, (**c**) O 1s, (**d**) Ca 2p and (**e**) Pd 3d.

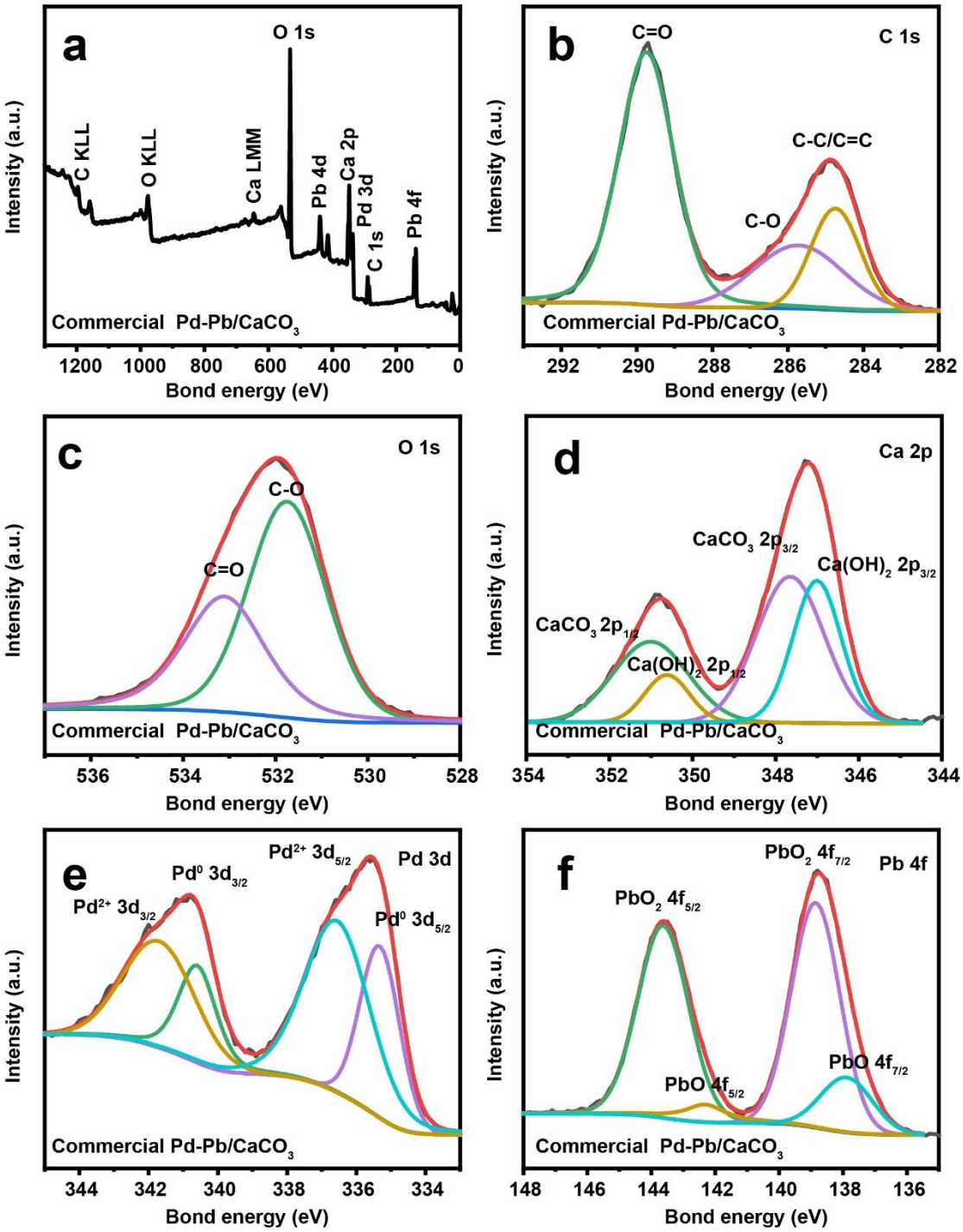

Figure S15. X-ray photoelectron spectroscopy (XPS) profiles of commercial Pd-Pb/$CaCO_3$ (i.e., Lindlar catalyst), including (**a**) full spectrum, (**b**) C 1s, (**c**) O 1s, (**d**) Ca 2p, (**e**) Pd 3d and (**f**) pb 4f.

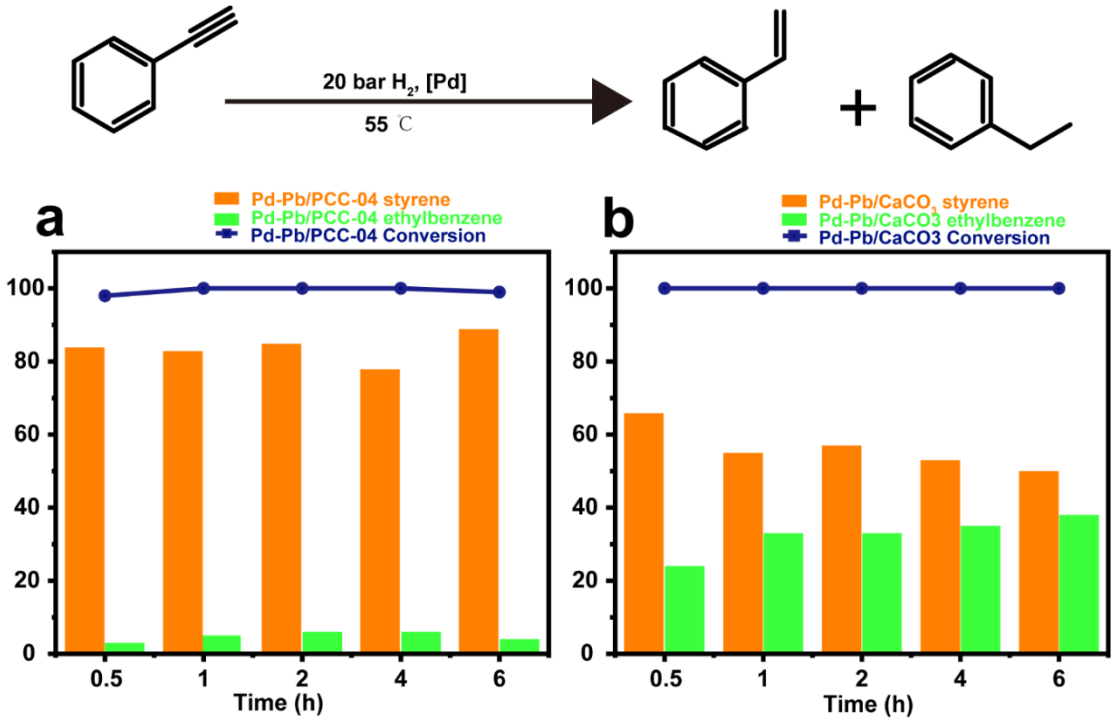

Figure S16. Time-monitored data of (**a**) 5 wt% Pd-Pb/PCC-04, and (**b**) 5 wt% Commercial Pd-Pb/$CaCO_3$ catalytic materials.

Section S2 | Supplementary Tables

Table S1. The catalyst screening with phenyl acetylene as a model substrate.[a]

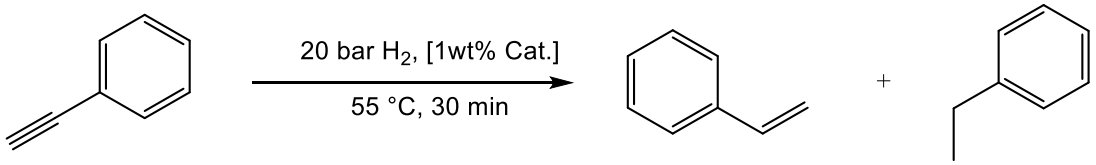

phenyl acetylene styrene ethylbenzene

Catalyst	Con. (%)	Styrene (%)	Ethylbenzene (%)
Pd/PCC-04	>99	1	92
Pd/PCC-30	>99	0	94
Pd/PCC-60	>99	0	93
Pd-Pb/PCC-04	>99	79	5
Pd-Pb/PCC-30	>99	69	13
Pd-Pb/PCC-60	>99	67	15

[a] Dimerized styrene has also been identified as a remaining product besides semi-hydrogenated styrene and fully-hydrogenated ethylbenzene.

Table S2. Comparison of semi-hydrogenation performance of alkyne over Pd-based catalysts.

Entry	Catalyst	Substrate	Temp. (℃)	Time (min)	Con. (%)	Alkene Sel. (%)	Ref.
1	20 mg, 5 wt% Pd–Pb/$CaCO_3$	4-phenylbut-3-yn-2-one	25	16	99	88	[10]
2	2 mg Quinoline, 20 mg, 5 wt% Pd–Pb/$CaCO_3$	4-phenylbut-3-yn-2-one	25	16	99	97	[10]
3	Pd_3Pb/SiO_2	4-phenylbut-3-yn-2-one	25	95	99	98	[10]
4	Pd_3Pb/SiO_2 and $RhSb/SiO_2$	4-phenylbut-3-yn-2-one	25	110	100	85	[10]
5	Pd_3Pb/SiO_2 and $RhSb/SiO_2$	4-phenylbut-3-yn-2-one	25	150	100	85	[10]
6	Pd_3Pb/SiO_2 and $RhSb/SiO_2$	4-phenylbut-3-yn-2-one	25	220	100	84	[10]
7	Pd_3Pb/SiO_2 and $RhSb/SiO_2$	4-phenylbut-3-yn-2-one	25	400	100	85	[10]
8	$Pd_{0.5}/CaCO_3$	Phenylacetylene	30	60	78	78	[16]
9	1% Pd/ND@G	Phenylacetylene	25	70	100	85.2	[26]
10	PdZn	ethylene	80	300	100	>90	[18]
11	Cu_3Pd_1/SN	Phenylacetylene	25	60	99.6	99.4	[22]
12	Ni/Pd (30:70)	phenylacetylene	50	285	100	97.3	[23]
13	Pd1–Fe/Fe_2O_3(012)	phenylacetylene	30	70	100	99.9	[24]
14	$Pd_{0.5}/\gamma$-Al_2O_3	phenylacetylene	25	20	98	94	[25]
15	UiO-67@Pd@UiO-67 (50 nm)	phenylacetylene	28	10	100	93.1	[36]
16	Pd^s–GDY	phenylacetylene	25	120	100	95.8	[37]
17	$PdIn/MgAl_2O_4$	diphenylacetylene	25	330	99	99	[38]
18	$PdIn/MgAl_2O_4$	$PdIn/MgAl_2O_4$	25	210	92	89	[38]
19	Lindlar catalyst	Phenylacetylene	20	120	65.7	50.7	[29]
20	Pd-Pb/PCC-04	Phenylacetylene	50	30	>99	81	This work